

## Mass Measurements beyond the Major $r$ -Process Waiting Point $^{80}\text{Zn}$

S. Baruah,<sup>1</sup> G. Audi,<sup>2</sup> K. Blaum,<sup>3,4,\*</sup> M. Dworschak,<sup>3</sup> S. George,<sup>3,4,\*</sup> C. Guénaut,<sup>2</sup> U. Hager,<sup>5,9,†</sup> F. Herfurth,<sup>3</sup> A. Herlert,<sup>1,‡</sup>  
A. Kellerbauer,<sup>6,\*</sup> H.-J. Kluge,<sup>3,7</sup> D. Lunney,<sup>2</sup> H. Schatz,<sup>8</sup> L. Schweikhard,<sup>1</sup> and C. Yazidjian<sup>3</sup>

<sup>1</sup>*Institut für Physik, Ernst-Moritz-Arndt-Universität, 17487 Greifswald, Germany*

<sup>2</sup>*CSNSM-IN2P3-CNRS, Université de Paris Sud, Orsay, France*

<sup>3</sup>*GSI, Planckstr. 1, 64291 Darmstadt, Germany*

<sup>4</sup>*Institut für Physik, Johannes Gutenberg-Universität, 55099 Mainz, Germany*

<sup>5</sup>*Department of Physics, University of Jyväskylä, P.O. Box 35 (YFL), 40014 Jyväskylä, Finland*

<sup>6</sup>*Physics Department, CERN, 1211 Geneva 23, Switzerland*

<sup>7</sup>*Fakultät für Physik und Astronomie, Ruprecht-Karls-Universität, 69120 Heidelberg, Germany*

<sup>8</sup>*Department of Physics and Astronomy, NSCL, and JINA, Michigan State University, East Lansing, Michigan 48824, USA*

<sup>9</sup>*Helsinki Institute of Physics, University of Helsinki, 00014 Helsinki, Finland*

(Received 12 September 2008; published 30 December 2008)

High-precision mass measurements on neutron-rich zinc isotopes  $^{71m,72-81}\text{Zn}$  have been performed with the Penning trap mass spectrometer ISOLTRAP. For the first time, the mass of  $^{81}\text{Zn}$  has been experimentally determined. This makes  $^{80}\text{Zn}$  the first of the few major waiting points along the path of the astrophysical rapid neutron-capture process where neutron-separation energy and neutron-capture  $Q$ -value are determined experimentally. The astrophysical conditions required for this waiting point and its associated abundance signatures to occur in  $r$ -process models can now be mapped precisely. The measurements also confirm the robustness of the  $N = 50$  shell closure for  $Z = 30$ .

DOI: 10.1103/PhysRevLett.101.262501

PACS numbers: 21.10.Dr, 26.30.-k, 27.50.+e

The rapid neutron-capture process ( $r$  process) is responsible for the synthesis of about half of the heavy elements beyond Ge in the cosmos [1–4]. However, where this process occurs is not known with certainty. The characteristic abundance patterns of various competing models not only depend on the chosen astrophysical environment, but also sensitively on the underlying nuclear physics processes and parameters [5–7]. Reliable nuclear data on the extremely neutron-rich nuclei participating in the  $r$  process are therefore needed to compare the signatures of specific models with astronomical data now emerging from observations of metal-poor stars [2]. Reliable nuclear physics is also needed to disentangle contributions from many different processes to the observed stellar abundance patterns below  $A = 130$ , which were previously attributed to the  $r$  process [8,9].

$\beta$ -decay half-lives and nuclear-mass differences along isotopic chains, i.e., neutron-separation energies, are of particular importance in  $r$ -process models, especially at the neutron-shell closures where the  $r$  process passes through the  $\beta$  decay of some particularly long-lived “waiting point” nuclei. The most prominent waiting points are believed to be  $^{80}\text{Zn}$ ,  $^{130}\text{Cd}$ , and probably  $^{195}\text{Tm}$ , responsible for producing the pronounced abundance peaks observed around mass numbers 80, 130, and 195, respectively. They serve as critical normalization points to constrain the conditions required to produce a successful  $r$  process [5].

$Q$ -value measurements related to these waiting points were performed only recently for  $^{130}\text{Cd}$  [10] using the  $\beta$ -endpoint technique and yielding a  $\beta$ -decay  $Q$ -value

with an uncertainty of 150 keV. While these results provide important new insights in nuclear structure and global mass models, their accuracy is not sufficient for  $r$ -process calculations. Furthermore, they may have large systematic uncertainties due to poorly known level schemes, which can result in rapidly increasing uncertainties as measurements are extended to more exotic nuclei. In addition, to constrain the path of the  $r$  process, neutron-separation energies and neutron-capture  $Q$ -values are needed, requiring mass measurements beyond the waiting point nuclei with an accuracy of the order of 10 keV.

In this Letter, we report important experimental input for  $r$ -process nuclear physics: precision Penning-trap mass measurements reaching the  $r$ -process path at the  $^{80}\text{Zn}$  major waiting point, including the first mass measurement of  $^{81}\text{Zn}$ . Penning-trap mass spectrometry has been developed in recent years for the use with radioactive beams. Continued refinements have enabled mass measurements with uncertainties of a few keV for increasingly exotic nuclei [11,12], which is important for astrophysics calculations. For example, Fig. 1 shows possible  $r$ -process reaction flows in the  $^{80}\text{Zn}$  region. Depending on the stellar conditions, the  $r$ -process path either includes the slow  $\beta$ -decay of  $^{80}\text{Zn}$  making it a waiting point, or proceeds rapidly via neutron capture to  $^{81}\text{Zn}$  and beyond. For some more extreme conditions,  $^{80}\text{Zn}$  can also be bypassed altogether. With the present measurements,  $^{80}\text{Zn}$  is the first major  $r$ -process waiting point where experimental values of the mass differences with respect to its neighbors ( $^{79}\text{Zn}$  and  $^{81}\text{Zn}$ ) are available, and thus a precise neutron-separation energy as well as a precise neutron-capture

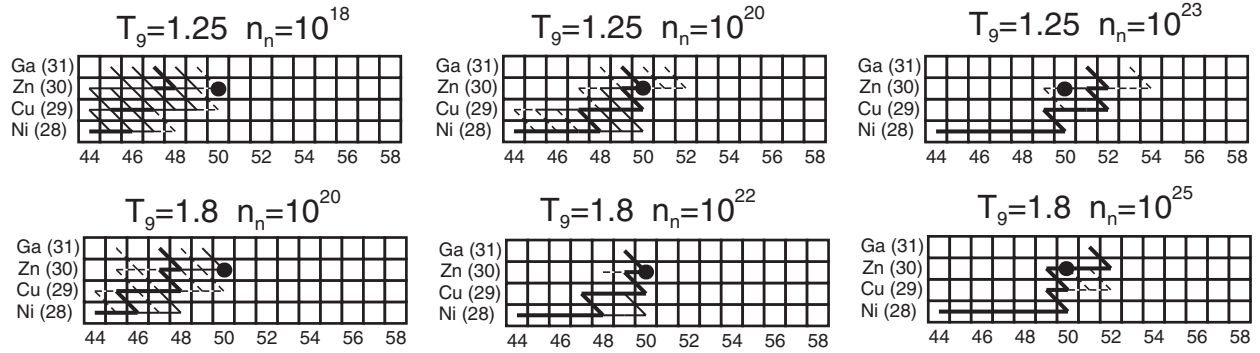


FIG. 1. Reaction flows in the  $^{80}\text{Zn}$  (black dot) region calculated in this work for various constant temperature and neutron-density conditions using the new nuclear masses obtained in this work. Thick lines denote reaction flows (time integrated abundance changes  $dY = dX/A$  with mass fraction  $X$  and mass number  $A$ ) in excess of  $5 \times 10^{-3}$ , while thin and dashed lines indicate reaction flows 1 or 2 orders of magnitude lower, respectively.

$Q$ -value. The conditions and role of  $^{80}\text{Zn}$  as a waiting point are discussed below.

The idea of a reduction of the strength of the closed neutron shell far from stability, discussed in the literature as “shell quenching,” has been evoked in the past in an attempt to explain some  $r$ -process abundance anomalies. However, evidence for this phenomenon in mass regions relevant for the  $r$  process has not been conclusive [10,13,14]. The very recent mass measurements of Hakala *et al.* [15] of neutron-rich Zn masses up to  $^{80}\text{Zn}$  at JYFLTRAP indicate that the  $N = 50$  shell strength is somewhat diminished down to  $Z = 31$ . Here, we provide some evidence that the  $N = 50$  shell closure is retained for the even more exotic case of  $Z = 30$ .

The masses of  $^{71m,72-81}\text{Zn}$  have been determined with the Penning-trap mass spectrometer ISOLTRAP [16] at ISOLDE, CERN. The radionuclides were produced by a 1.4-GeV proton pulse from the CERN Proton Synchrotron Booster with  $3 \times 10^{13}$  protons impinging every 2.4 s on a uranium-carbide target. In order to suppress a contamination by isobaric Rb isotopes, several techniques have been used: First, the protons were focussed on a neutron converter, i.e., a tungsten rod mounted next to the target container, thus enhancing neutron-induced fission and reducing direct nuclear reactions of protons with the actinide material. Second, further suppression of the alkali-metal isotopes was achieved by introducing a quartz tube into the transfer line between the target container and the ion source [17]: Rb isotopes diffusing out of the heated target container freeze out on the surface of the quartz, while the ions of interest pass unimpeded to the ionization region. Third, the atoms were selectively ionized by resonant laser ionization [18]. In total, a suppression factor for  $^{80}\text{Rb}$  of the order of  $10^4$  was achieved at a quartz temperature of  $680^\circ\text{C}$  [17].

The Zn ions were accelerated to 60-keV kinetic energy and further purified by the high resolution mass separator HRS before being transferred to the ISOLTRAP setup. The ions were stopped in a helium-gas-filled linear radiofrequency quadrupole (RFQ) ion trap. The ion bunch was

transferred to the first Penning trap for the removal of any isobaric contamination still present [19]. Finally, the purified bunch of zinc ions was sent to the precision Penning trap, where the cyclotron frequency  $\nu_c = qB/(2\pi m)$  is measured with the well-established time-of-flight ion cyclotron-resonance technique [20].

In addition to isobaric cleaning, *isomeric purification* by resonant dipolar rf excitation [21,22] was used in the precision trap in order to perform measurements on clean ion ensembles. For  $^{77}\text{Zn}$ , an admixture of the excited  $^{77m}\text{Zn}$  ( $\Delta E = 772.4$  keV) needed to be removed [23] to measure the cyclotron frequency of the ground state  $^{77}\text{Zn}^+$ . In the case of  $^{71}\text{Zn}$ , the isomer was much more abundant than the ground state, and therefore the cyclotron frequency of  $^{71m}\text{Zn}^+$  was measured after removing any remaining  $^{71}\text{Zn}^+$  ions. The determination of the cyclotron frequencies and the frequency ratios  $r = \nu_{c,\text{ref}}/\nu_c$  of the reference ion  $^{85}\text{Rb}^+$  and the ion of interest with the respective uncertainties follows the procedure described in [24]. All present uncertainties for the frequency ratios are governed by the statistical uncertainties of the  $\nu_c$  measurements, which are of the order of a few times  $10^{-8}$ . For  $^{81}\text{Zn}$ , with a half-life of only 0.3 s, the mass has been measured for the first time and a relative mass uncertainty below  $7 \times 10^{-8}$  has been achieved. The recent mass values of  $^{76-80}\text{Zn}$  measured by JYFLTRAP [15] are in excellent agreement.

In Table I, the resulting mass excess values are given. Some of them deviate from the AME2003 literature values [25], especially  $^{73}\text{Zn}$ , by more than 4 standard deviations. Therefore, the present frequency ratios have been taken as input values for a new mass evaluation. A new estimate for the mass excess of  $^{82}\text{Zn}$  was derived from the systematic trends of the mass surface in that region of the nuclide chart. With  $\text{ME} = -42860(500)$  keV, it is shifted by  $-400$  keV as compared to the former estimated literature value [25].

Figure 2 shows the new neutron-separation energies in the Zn isotopic chain as a function of neutron number together with predictions from global mass models. The new data lead to accurate neutron-separation energies

TABLE I. Experimental frequency ratios  $r = \nu_{c,\text{ref}}/\nu_c$  of  $\text{Zn}^+$  ions relative to  $^{85}\text{Rb}^+$ . The mass excess  $\text{ME} = (m - A)m_u$  (with mass number  $A$  and mass  $m$  in atomic mass units) has been deduced from the mass  $m = r(m_{\text{ref}} - m_e) + m_e$  using the conversion factor  $m_u = 931494.0090(71)$  keV, the mass of  $^{85}\text{Rb}$   $m_{\text{ref}} = 84.911789738(12)$  u, and the mass of the electron  $m_e = 548579.9110(12) \times 10^{-9}$  u [25].

Nuclide	frequency ratio $r$	mass excess expt. $\delta m/m \times 10^{-8}$ (keV)	
$^{71}\text{Zn}$	0.835 311 546 0(302)	-67 171.2(2.4)	3.6
$^{72}\text{Zn}$	0.847 076 232 7(268)	-68 145.4(2.1)	3.2
$^{73}\text{Zn}$	0.858 885 502 0(236)	-65 593.4(1.9)	2.7
$^{74}\text{Zn}$	0.870 660 440 8(315)	-65 756.7(2.5)	3.6
$^{75}\text{Zn}$	0.882 477 875 0(245)	-62 558.9(1.9)	2.8
$^{76}\text{Zn}$	0.894 258 121 1(232)	-62 302.5(1.8)	2.6
$^{77}\text{Zn}$	0.906 079 544 4(287)	-58 789.1(2.3)	3.2
$^{78}\text{Zn}$	0.917 873 056 2(350)	-57 483.4(2.8)	3.8
$^{79}\text{Zn}$	0.929 701 243 6(490)	-53 435.1(3.9)	5.3
$^{80}\text{Zn}$	0.941 500 837 5(355)	-51 648.3(2.8)	3.8
$^{81}\text{Zn}$	0.953 346 729 7(632)	-46 199.6(5.0)	6.6

across the  $N = 50$  shell gap and show that the strength of the  $N = 50$  shell closure is maintained for Zn. This is in agreement with the recent study of the  $N = 50$  shell gap evolution [15] and extends its validity. Amongst the mass models, the finite range droplet model (FRDM) [26] shows the best agreement with the data, and there is no indication of a reduction of the  $N = 50$  shell gap relative to this model. The new HFB-14 mass model [27] also fits the data reasonably well. The ETFSI-Q mass model [28] that had been developed to explore possible effects of shell quenching clearly disagrees with the data.

For the subset of  $r$ -process models that are characterized by a neutron-capture flow through the  $N = 50$  mass region, the new results allow one to determine the astrophysical

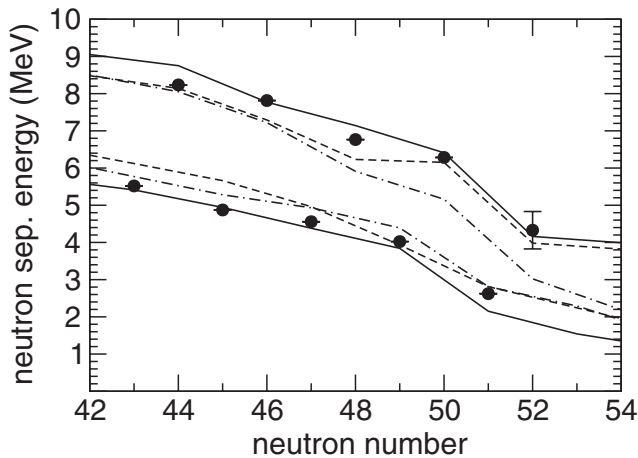


FIG. 2. Neutron-separation energies for neutron-rich Zn isotopes as functions of neutron number for the FRDM (solid line) [26], HFB-14 (dashed line) [27], and ETFSI-Q (dot-dashed line) [28] mass models together with the measured data from this work (black dots).

conditions for which  $^{80}\text{Zn}$  is a waiting point, therefore producing an  $A = 80$  abundance peak. To that end, we carried out dynamical reaction network calculations in the  $^{80}\text{Zn}$  region without the assumption of  $(n, \gamma) \rightleftharpoons (\gamma, n)$  equilibrium. The network includes isotopes from  $N = 44$  to 56 and elements from  $Z = 28$  to 31.  $(n, \gamma)$  reaction rates are taken from the statistical model NON-SMOKER [29] using the FRDM mass model [26]. The reverse  $(\gamma, n)$  reactions depend exponentially on neutron-separation energies and are calculated using the detailed balance principle (see [1] Eq. 4.5) with our new Zn mass values and partition functions based on the same level densities and spin assignments as in NON-SMOKER. With this approach, we neglect the mass dependence of the  $(n, \gamma)$  reaction rates themselves. This is justified with respect to the inherent uncertainty in the predicted rates. In addition, for most of the relevant conditions, the  $r$  process is dominated at least locally by  $(n, \gamma) \rightleftharpoons (\gamma, n)$  equilibria where the resulting reaction flows only depend on masses and partition functions, not on the reaction rates themselves.  $\beta$ -decay rates are taken from experiment when available [25,30]; otherwise, we use the predictions from a global quasiparticle random phase approximation (QRPA) calculation [31].

We start with an initial composition of  $^{72}\text{Ni}$  and neutrons only and run the network at a constant temperature and neutron density until all the abundance is accumulated at  $N = 56$ . Figure 1 shows some of the results. We then determine the fraction of the total reaction flow that has passed through the  $\beta$ -decay of  $^{80}\text{Zn}$  for such conditions. To account for mass uncertainties, we run for each temperature and neutron-density multiple calculations for all possible permutations where the Zn isotope masses are either set to their lower or their upper  $1\sigma$  limit. From this, we obtain the minimum and the maximum fraction of flow through the  $^{80}\text{Zn}$   $\beta$ -decay as a function of the temperature  $T_9$  and the neutron density  $n_n$ . Contours for 90%  $\beta$ -decay branching are used to define the conditions under which  $^{80}\text{Zn}$  is a waiting point.

Figure 3 shows the results for the 2003 atomic mass evaluation AME2003 [25] and the new experimental data. Clearly, the mass uncertainties of 200–500 keV in the AME2003 extrapolations for the isotopes around  $^{80}\text{Zn}$  translate into uncertainties of several orders of magnitude in neutron density and 0.2–0.4 GK in temperature. With our new data, in particular, with the first precision mass value of  $^{81}\text{Zn}$ , the picture changes drastically, and we now have a well defined map of conditions for a major  $r$ -process waiting point to be on the reaction path. This provides a first reliable guide for  $r$ -process models with neutron capture in this mass region. Model conditions need to pass through our defined region of temperature and neutron density in order to produce the observed high  $A = 80$  abundance.

Figure 3 shows two distinct temperature regimes above and below about 1.5 GK with different temperature and density dependencies and different sensitivities to mass

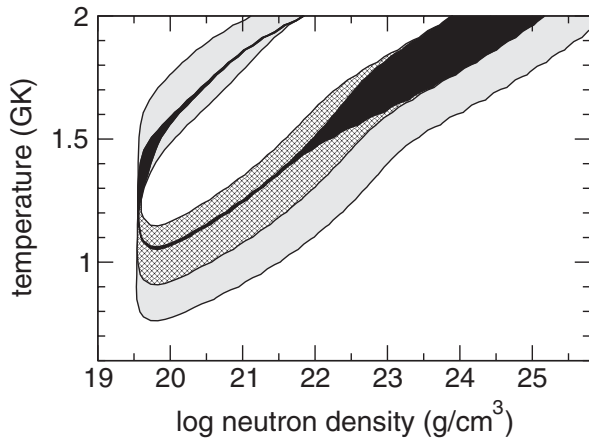


FIG. 3. Boundaries enclosing the temperature and neutron-density conditions required for an  $r$  process to produce a strong  $A = 80$  abundance peak. The black area indicates the result with mass values from this work. The thickness of the boundary indicates the remaining mass-related uncertainty. The cross-hatched area indicates the additional uncertainty without an improved mass value for  $^{81}\text{Zn}$ . The gray area indicates the additional mass uncertainty when using the AME2003 mass values [25].

uncertainties. Above 1.5 GK ( $n, \gamma \rightleftharpoons \gamma, n$ ), equilibrium is fully established and even- $N$  isotopes play the dominant role because of their higher neutron-separation energies. In this regime, the calculations are expected to be insensitive to neutron-capture rates. Additional uncertainties from partition functions should be small as well, as the even- $N$  isotopes are even-even nuclei with ground state spin zero, and with a relatively low level density on excitation energy scales corresponding to the few 100 keV of thermal energy. The largest remaining uncertainty in this regime is the mass of  $^{82}\text{Zn}$ , which governs the leakage out of  $^{80}\text{Zn}$ . While our measurements have improved the mass extrapolation for  $^{82}\text{Zn}$ , a precision measurement would be desirable.

For temperatures below 1.5 GK, ( $n, \gamma \rightleftharpoons \gamma, n$ ) equilibrium begins to break down. For the high neutron-density boundary, leakage out of  $^{80}\text{Zn}$  is governed by a local equilibrium between  $^{80}\text{Zn}$  and  $^{81}\text{Zn}$ , followed by neutron capture on  $^{81}\text{Zn}$ . The most critical quantity in this regime is the mass difference between  $^{80}\text{Zn}$  and  $^{81}\text{Zn}$ , which we have determined here experimentally for the first time, making the previously dominating mass uncertainties negligible. For the low neutron-density boundary, the reaction flow is determined by competition between  $\beta$ -decay and neutron capture and becomes insensitive to masses as Fig. 3 shows. For this low-temperature regime, predictions of neutron-capture rates and partition functions might contribute small additional uncertainties.

This work was supported by the German Federal Ministry for Education and Research (06GF151 and 06MZ215), by the European Commission (NIPNET RTD

network HPRI-CT-2001-50034), and by the Helmholtz association for research centers (VH-NG-037). H. S. is supported by NSF Grants No. PHY0606007 and No. PHY0216783. S.B. thanks the University of Greifswald for a grant in the framework of the International Max Planck Research School. We thank the ISOLDE Collaboration and the technical team for their support.

\*Present address: Max-Planck-Institut für Kernphysik, Saupfercheckweg 1, 69117 Heidelberg, Germany.

†Present address: TRIUMF, 4004 Wesbrook Mall, Vancouver, British Columbia, V6T 2A3, Canada.

‡Present address: CERN, Physics Department, 1211 Geneva 23, Switzerland.

- [1] J. J. Cowan, F.-K. Thielemann, and J. W. Truran, *Phys. Rep.* **208**, 267 (1991).
- [2] J. W. Truran *et al.*, *Publ. Astron. Soc. Pac.* **114**, 1293 (2002).
- [3] Y.-Z. Qian, *Prog. Part. Nucl. Phys.* **50**, 153 (2003).
- [4] M. Arnould *et al.*, *Phys. Rep.* **450**, 97 (2007).
- [5] K.-L. Kratz *et al.*, *Astrophys. J.* **403**, 216 (1993).
- [6] B. Chen *et al.*, *Phys. Lett. B* **355**, 37 (1995).
- [7] S. Wanajo *et al.*, *Astrophys. J.* **606**, 1057 (2004).
- [8] C. Travaglio *et al.*, *Astrophys. J.* **601**, 864 (2004).
- [9] F. Montes *et al.*, *Astrophys. J.* **671**, 1685 (2007).
- [10] I. Dillmann *et al.*, *Phys. Rev. Lett.* **91**, 162503 (2003).
- [11] K. Blaum, *Phys. Rep.* **425**, 1 (2006).
- [12] Special issue on Ultra-accurate mass spectrometry and related topics, edited by L. Schweikhard and G. Bollen, [*Int. J. Mass Spectrom.* **251**, Nos. 2-3 (2006)].
- [13] M. Dworschak *et al.*, *Phys. Rev. Lett.* **100**, 072501 (2008).
- [14] A. Jungclaus *et al.*, *Phys. Rev. Lett.* **99**, 132501 (2007).
- [15] J. Hakala *et al.*, *Phys. Rev. Lett.* **101**, 052502 (2008).
- [16] M. Mukherjee *et al.*, *Eur. Phys. J. A* **35**, 1 (2008).
- [17] E. Bouquerel *et al.*, *Eur. Phys. J. Special Topics* **150**, 277 (2007).
- [18] V. I. Mishin *et al.*, *Nucl. Instrum. Methods Phys. Res., Sect. B* **73**, 550 (1993).
- [19] K. Blaum *et al.*, *J. Phys. B* **36**, 921 (2003).
- [20] G. Gräff *et al.*, *Z. Phys. A* **297**, 35 (1980).
- [21] K. Blaum *et al.*, *Europhys. Lett.* **67**, 586 (2004).
- [22] J. Van Roosbroeck *et al.*, *Phys. Rev. Lett.* **92**, 112501 (2004).
- [23] A. Herlert *et al.*, *Czech. J. Phys.* **56**, F277 (2006).
- [24] A. Kellerbauer *et al.*, *Eur. Phys. J. D* **22**, 53 (2003).
- [25] G. Audi *et al.*, *Nucl. Phys. A* **729**, 3 (2003).
- [26] P. Möller *et al.*, *At. Data Nucl. Data Tables* **59**, 185 (1995).
- [27] S. Goriely, M. Samyn, and J. M. Pearson, *Phys. Rev. C* **75**, 064312 (2007).
- [28] J. M. Pearson *et al.*, *Phys. Lett. B* **387**, 455 (1996).
- [29] T. Rauscher and F. K. Thielemann, *At. Data Nucl. Data Tables* **75**, 1 (2000).
- [30] P. Hosmer *et al.*, *Phys. Rev. Lett.* **94**, 112501 (2005).
- [31] P. Möller, J. R. Nix, and K.-L. Kratz, *At. Data Nucl. Data Tables* **66**, 131 (1997).